Soliton based Dynamic Nuclear Polarization:

Overhauser effect in cyclic polyacetylene at high field and room temperature

Z. Miao, ¹ F. J. Scott, ² J. van Tol, ² C. R. Bowers, ^{1, 2} A. S. Veige, ¹ F. Mentink-Vigier*²

¹Department of Chemistry, University of Florida, Center for Catalysis, Gainesville, FL, USA

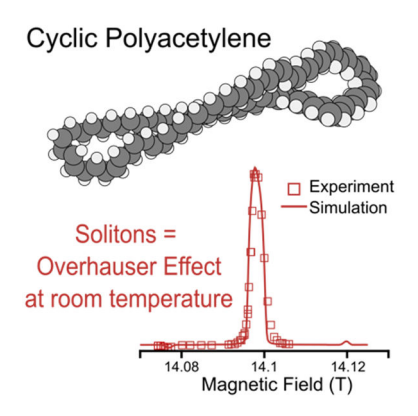
²National High Magnetic Field Laboratory, Florida State University, 1800 E. Paul Dirac Dr, 32310, Tallahassee, FL, USA

^{*} Frederic Mentink-Vigier: fmentink@magnet.fsu.edu

ABSTRACT

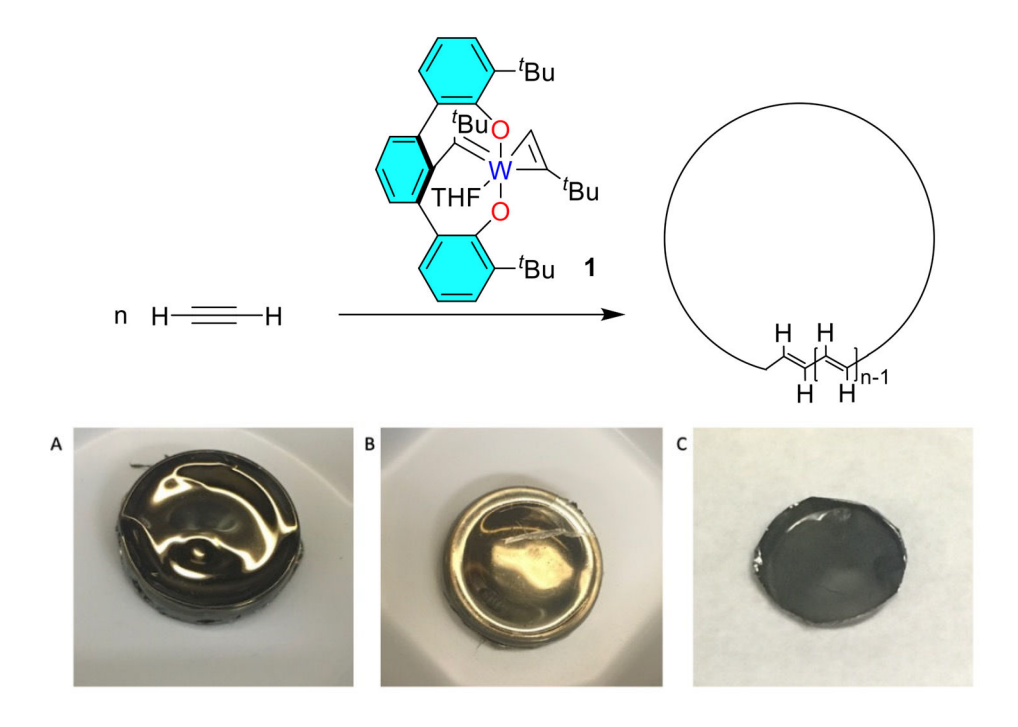
Polyacetylene, a versatile material with an electrical conductivity that can span seven orders of magnitude, is the prototypical conductive polymer. In this letter, we report the observation of a significant Overhauser Effect at the high magnetic field of 14.1 T that increases with temperature in both linear and cyclic polyacetylene. Significant NMR signal enhancements ranging from 24 to 45 are obtained. The increased sensitivity enabled the characterization of the polymer chain defects at natural abundance. The absence of end methyl group carbon-13 signals provides proof of the closed-loop molecular structure of the cyclic polyacetylene. The remarkable efficiency of the soliton based Overhauser Effect DNP mechanism at high temperature and high field holds promise for applications and extension to other conductive polymer systems.

TOC GRAPHICS



KEYWORDS EPR, cyclic polymer, conductive polymer, NMR, Magic Angle Spinning, MAS-DNP

In recent years, the research and utilization of conductive polymers has expanded significantly, with applications ranging from optoelectronics to material science. Linear polyacetylene (linear PA), the simplest polyene and the most extensively studied organic conjugated polymer, was first synthesized using titanium-based catalysts by Natta in 1958. A major breakthrough occurred when Shirakawa synthesized free standing films of linear PA, endowing PA materials with both mechanical flexibility as a polymer film^{3,4} and, after doping, conductivities comparable to metals. When synthesized at -78 °C using Shirakawa's method, linear PA contains *cis* double bonds as a natural consequence of an insertion mechanism but the more stable *trans-transoid* isomer with higher conductivities can be obtained via thermal isomerization. In 2022, we reported the synthesis of cyclic polyacetylene (cyclic PA; Figure 2). Unique to its topology, cyclic PA synthesized with catalyst 1^{11–15} (Scheme 1) exhibits an exclusively *trans-transoid* structure, even at -94 °C.



Scheme 1. Synthesis of cyclic polyacetylene with catalyst 1. Panels A-C depicts various samples of cyclic polyacetylene that can be produced with catalyst 1.

Characterizing such a conductive polymer is a challenge because it is insoluble. For such materials, solid-state NMR provides unrivaled structural information at the atomic scale. However, conventional solid-state NMR is a notoriously insensitive technique which makes it challenging to detect chemical sites at low concentrations. The sensitivity of solid-state NMR can be increased by combining magic angle spinning (MAS) with Dynamic Nuclear Polarization (DNP). DNP increases the nuclear spin polarization via irradiation of electron spin resonance transitions associated with paramagnetic centers with a high power microwave source. 16-21 With only a few notable exceptions, 22-24 MAS-DNP in high magnetic fields is carried out with extrinsic paramagnetic species at low temperature where the electron and nuclear spin dynamics is more favorable.^{25–27} DNP using intrinsic paramagnetic species is interesting as it directly probes the properties, spin interactions, and spin dynamics of the material itself.^{28–30} In this context, conductive polymers are intriguing materials for fundamental studies of high-field MAS-DNP that can server as a unique probe of structure and dynamics in solids with extended electronic states. Among conductive polymers, linear PA is known to display efficient Overhauser effect (OE) DNP at low fields ranging from 0.3 to 1.4 T using the bond alternation domain wall (a.k.a. solitons³¹) and trapped unpaired electron spins.^{32–35} However, DNP at high field on conductive samples is challenging. It requires the sample to be sufficiently transparent to uw irradiation, but since the skin depth in conductors is inversely proportional to the µw frequency, the volume that is effectively irradiated is limited, and microwave absorption can result in significant sample heating, even for materials with modest conductivity.³⁶ In addition, the dynamic properties of the spin system, particularly the spectral density of the fluctuations in the electron-nuclear coupling at the

Larmor frequency difference frequency, needs to be sufficient to generate DNP at high field, which is one of the key challenges of OE in liquids.^{37,38} Therefore, reports of room temperature MAS-DNP in paramagnetic organic materials at high field are rare, and to our knowledge, DNP in a conductive organic solid at high magnetic field (≥14.1 T) has not been previously reported.

In this letter we report the unexpectedly strong ¹H MAS-DNP signal enhancements ranging between 24 and 45 in both undoped linear and cyclic polyacetylene (*trans-transoid*),³⁹ hereafter referred to as linear PA and cyclic PA, at high field and room temperature. The explanation of the origin of these remarkable signal enhancements is guided by previous studies on linear PA^{32–35} together with EPR spectroscopy and numerical simulations based on the Overhauser (OE) and Solid Effect (SE) mechanisms. These large enhancements enabled us to analyze the topological and chemical defects in the novel cyclic conductive polymer.³⁹ The quality of the data suggests that the method is extensible to other conductive polymers.^{1,40}

Conductive polymers such as polyacetylene contain defects in the π -conjugation that are referred to as bond alternation domain-walls or solitons³¹ that bear isolated unpaired electrons.⁴⁰ The conduction mechanism is different than in metals as it relies on the presence of these electronic defects with energy levels in the band-gap as in semiconductors. Here, the linear and cyclic PA samples were initially characterized by EPR. The room temperature X-band EPR spectra (9.6 GHz / 0.3 T) presented in Fig. S1 of the Supporting Information (S.I.) exhibit a single, featureless resonance reflecting the high mobility of the conduction electrons which averages the local spin interactions,^{41,42} i.e., the g-tensor and hyperfine couplings. The EPR linewidth is 0.12 mT for the linear PA (similar to previous reports)³² and 0.2 mT for cyclic PA. The motional narrowing indicates that the correlation time is much shorter than the inverse of the largest hyperfine coupling.

 $\frac{1}{|A|_{\text{max}}} \approx \frac{1}{12 \text{ MHz}}^{42}$ with an upper bound of $\sim 10^{-13} \text{ s}, \frac{32,33,35,43}{12 \text{ consistent}}$ consistent with the literature reports for linear PA^{33,41}. The high-field EPR spectra at 8.4 T/240 GHz at a series of different temperatures are presented in Figure 1. In both samples, the EPR transition broadens as the temperature is reduced from 220 K to 10 K. At this field, the low temperature EPR linewidths for linear and cyclic PA at 100 K are 1.64 mT and 1.27 mT, respectively, considerably larger than at X-band. 32 At high field, the effect of g-tensor anisotropy on the EPR spectra is more important, and motional narrowing is not as effective. Fits of the EPR spectra for both samples at 100 K and 10 K using a single spin population are reported in Fig. S5. While at 100 K the agreement is reasonable, it is poor at 10 K, especially for the linear PA. Indeed, the EPR spectra of the linear PA sample exhibits additional features at 10 K, as does the cyclic PA to a lesser extent. This observation aligns with the existing literature, suggesting the presence of two distinct spin populations in linear PA: one comprised of delocalized electron spins that move along the chain and another consisting of electrons trapped in localized defects. 32,33,35,40,44 As the temperature decreases, the delocalized electrons become trapped within the defect sites, leading to reduced motional narrowing. 32,33,41,42,44 In linear PA, the exact nature of the defect sites is debated; they could arise from either O₂ exposure^{32,33} or residual *cis* bonds. ⁴³ The soliton mobility in cyclic PA follows the same trend. The EPR line exhibits some asymmetry as the temperature is lowered, also indicating reduced motional narrowing. However, at 10 K the EPR linewidth of cyclic PA is only that of the linear PA line and presents fewer features. This suggests that the reduction in mobility within cyclic PA is less pronounced. This is consistent with a lower density of topological (e.g. cis bonds) and polymer chain defects in the cyclic PA sample and/or a soliton trapping potential that is shallower compared to that of the linear PA sample. 32,35,45

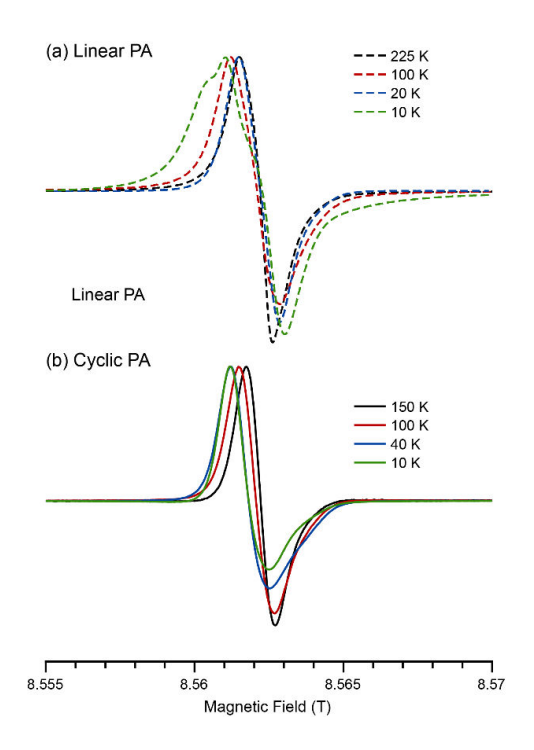


Figure 1 EPR spectra as a function of temperature of (a) linear PA and (b) cyclic PA collected between 225 K and 10 K at a μw frequency of 240 GHz.

MAS-DNP NMR experiments were performed on linear and cyclic PA samples at magnetic fields around 14.1 T or 600 MHz 1 H Larmor frequency. Figure 2 (a) presents plots of the 1 H NMR signal enhancements as a function of the static magnetic field for a fixed microwave frequency of 395.145 GHz at 100 K. Both samples exhibit maximum enhancement of the 1 H nuclear spin polarization for microwave irradiation (μ w) at the EPR resonance condition. Significant enhancements of 24 and 32 were obtained for linear PA and cyclic PA, respectively. In addition, a modest nuclear spin depolarization is observed at the lower field of 14.078 T. The sign of the enhancement remains constant in the vicinity of ~14.095 T which is characteristic of the Overhauser Effect (OE) mechanism. $^{46-48}$ In addition, the maximum enhancement is obtained for a modest μ w irradiation strength (~8 W at 100 K, see Fig. S2) while the depolarization at ~14.078 T (\equiv 600 MHz lower Larmor Frequency) is attributed to the SE^{49,50} mechanism where irradiation

of the double quantum electron-nucleus transition generates a polarization below thermal equilibrium.

As seen in Figure 2(a), the enhancement due to the OE in cyclic PA is significantly larger than the SE enhancment, as it reaches 32 while for the SE it is only ~0.6. For the linear PA sample, the OE enhancement is as high as 24 but only 0.7 for the SE condition. The observation of the OE indicates a fast fluctuation of the isotropic hyperfine couplings with an upper limit on the correlation time of $1/(2\pi \times 395 \text{ GHz}) \approx 4.10^{-13} \text{ s}$ that can be attributed to the soliton dynamics. 32,35,51 Nevertheless, the identification of the SE DNP mechanism implies that the anisotropic hyperfine coupling is not entirely averaged at 100 K. Again, this suggests that either the motional averaging resulting from electron spin delocalization is incomplete or there are two distinct populations of unpaired electron spins. The former assertion aligns with experimental findings in linear PA32,33,35,44,52 as well as the high field EPR spectra. Hence, it is reasonable to extend this interpretation to cyclic PA. Since the two electron spin populations have identical Larmor frequencies, the enhancement field profile was simulated by considering the coupling between N nuclear spins and n electron spins split into two populations, n_1 on site #1 and n_2 on site #2. The coupling for both should be temperature dependent. The corresponding rotating frame spin Hamiltonian is given by:

$$\begin{split} \hat{H}_{0} &= \sum_{l=1}^{n} ((g\beta B_{0} - \Delta\omega)\hat{S}_{z,l} + \omega_{1}\hat{S}_{x,l} \\ &+ \sum_{k=1}^{N} \left(\sum_{l=1}^{n_{1}} A_{z,l,k}^{\mathrm{iso}} \hat{S}_{z,l} \hat{I}_{z,k} \right. \\ &+ \sum_{m=1}^{n_{2}} + 2A_{z,m,k}^{\mathrm{aniso}} \hat{S}_{z,m} \hat{I}_{z,k} + A_{+,m,k}^{\mathrm{aniso}} \hat{S}_{z,m} \hat{I}_{+,k} + A_{-,m,k}^{\mathrm{aniso}} \hat{S}_{z,m} \hat{I}_{-,k} \right) \end{split}$$
 Eq. (1)

The first two terms relate to the Zeeman and μ w interactions, while the remaining terms represent the hyperfine couplings to the nuclei. We assume that the nuclei are equilibrating quickly and thus

can be represented as a single nucleus. Since the two mechanisms are well separated in frequency, the problem can be reduced to a simple "two-spin" system where only the "average" hyperfine couplings are considered for each of the two populations:

$$\widehat{H}_{0} = (g\beta B_{0} - \Delta\omega)\widehat{S}_{z} + \omega_{1}\widehat{S}_{x}
+ \widehat{S}_{z} (\langle 2A_{z}^{\text{iso}} + A_{z}^{\text{aniso}} \rangle \langle \widehat{I}_{z} \rangle + \langle A_{+}^{\text{aniso}} \rangle \langle \widehat{I}_{+} \rangle + \langle A_{-}^{\text{aniso}} \rangle \langle \widehat{I}_{-} \rangle)$$
Eq. (2)

Under this approach, $\langle A_Z^{\rm iso} \rangle$ and $\langle A_{Z/\pm}^{\rm aniso} \rangle$ should be temperature dependent as they depend on the relative site populations n_1 and n_2 . The simulations of the field profile used the fitted g-values at 100 K and the measured intrinsic nuclear spin-lattice relaxation times (0.45 for linear PA and 0.5 s for cyclic PA sample #2). From these relaxation times, and DFT simulations reported in the SI, it is possible to extract the Zero Quantum (ZQ) and Double Quantum (DQ) relaxation rates, assuming a 1D diffusion of the solitons with a diffusion coefficient, $D_{f/f}$. The simulations of the OE and SE are reported in Figure 2 (a) as dashed lines, and the previously reported electron spin relaxation time for linear PA (0.1 ms). The only fitting parameter is $\langle A_{\Box}^{\rm aniso} \rangle$ that we found to be 0.2 MHz, in good agreement with the SE experiments. The agreement between experiments and simulations for the OE is very good for the cyclic PA and good for the linear PA. The maximum enhancement is well reproduced for the cyclic PA and slightly overestimated for the linear PA. The relaxation model previously developed PA and slightly overestimated for the linear PA. The relaxation model previously developed PA and slightly overestimated for the linear PA. The relaxation model previously developed PA and slightly overestimated for the linear PA. The relaxation model previously developed PA and slightly overestimated for the linear PA. The relaxation model previously developed PA and slightly overestimated for the linear PA. The relaxation model previously developed PA and slightly overestimated for the linear PA. The relaxation model previously developed PA and SI should be PA and SI

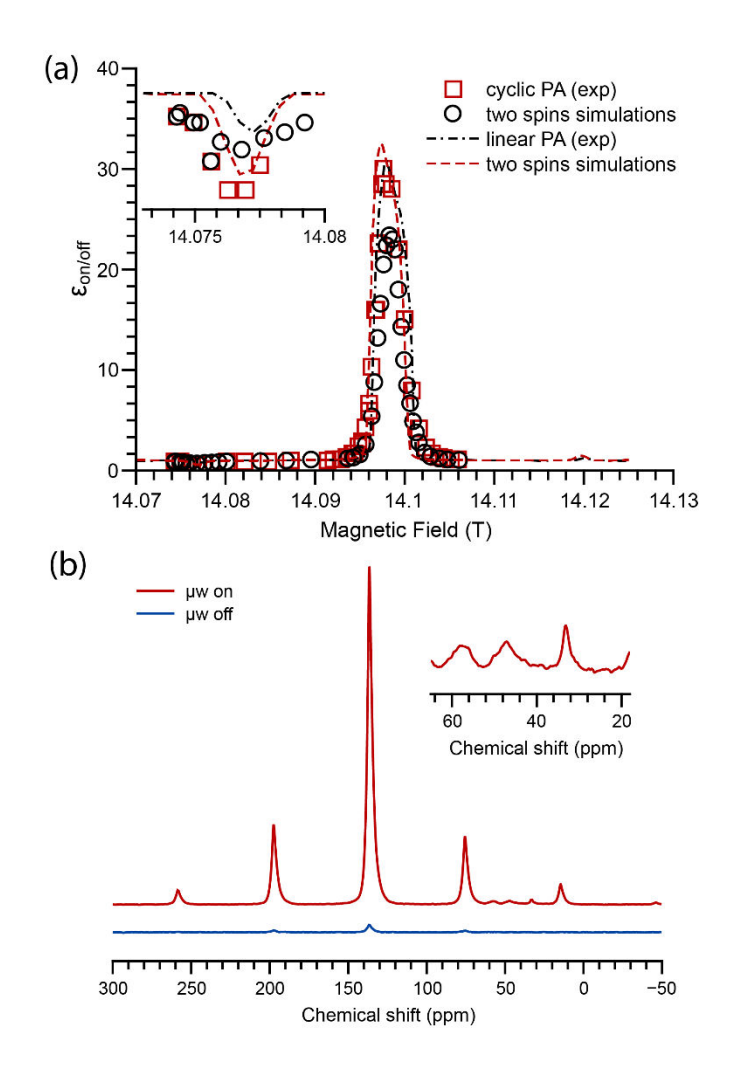


Figure 2 (a) ¹H MAS-DNP field profiles for linear PA (black circles) and cyclic PA (red squares, sample #2) collected at 100 K and 9.2 kHz spinning speed and the corresponding simulated enhancement using the two-spin model (dashed line, same colors) of Eq. (2). The insert is a focused view of the Solid-Effect negative (DQ) enhancement region. (b) ¹H→¹³C CP spectra of cyclic PA (sample #1) collected at room temperature with (red) and without (blue) μw irradiation (19 W, see SI). A focused view of the cyclic PA polymer chemical defect region is displayed in the insert.

The OE DNP mechanism was further explored by measuring the ¹³C enhancement due to direct polarization (see Table 1). At 100 K, it is of the same order of magnitude as the ¹H enhancement.

Nuclear spin diffusion between ¹³C nuclei at natural isotopic abundance is negligible; hence, the observed large enhancement values confirm that the solitons are well delocalized over the chains.

Table 1: Measured values of the 1 H and 13 C polarization enhancements $\epsilon_{\rm on/off}$ and build-up times T_B for linear PA and cyclic PA. Note that the build-up time for the 13 C sample is not purely mono-exponential, and the reported T_B is the approximate time scale.

OE ¹ H	OE ¹³ C (direct)

	$\epsilon_{ m on/off}$		T_B		$\max \epsilon_{\mathrm{on/off}}$	T_B
Sample	100 K	290 K	100 K	290 K	100 K	
Linear PA	24	26	0.45 s	0.3	~20	32 s
Cyclic PA sample #1	30	45	1 s	0.5 s	~30	90 s
Cyclic PA sample #2	32	38	0.5 s	0.26 s	~48	-

Previous publications in the 1980s on linear *trans*-PA reported proton polarization enhancements with OE DNP at room temperature. However, most of the experiments were carried out at low fields $(B_0 \le 1.4 \text{ T})^{34,35,53,54}$ where conditions are much more favorable for DNP in a conductive material (*vide supra*) but resulted in low resolution NMR spectra. As reported in table 2, we found that the DNP enhancement in cyclic PA at 100 K exceeds that of linear PA at 14.1 T, and furthermore, the enhancement in the former is even greater at room temperature (RT). At room temperature, cyclic PA exhibits a large enhancement at the optimal OE position. This enhancement increases from ~30 at 100 K to 45 at RT for both samples tested. At RT, the buildup times are faster, yet the enhancements are higher. The shortening of the nuclear relaxation times by a factor 2 can be explained by the relaxation models in a 1D chain that should lead to a linear dependence $\frac{1}{T_{1,n}} \propto \frac{n_1(T)T}{\sqrt{D_f}/f}$ (see SI). The increased enhancements at RT can be due to an increase in the number

of spins that generates OE, in other words $n_1(T)$ increases and $n_2(T)$ decreases which in turns increases the number of nuclei that undergo OE. This further supports our hypothesis for the existence of two populations of solitons in cyclic PA: the mobile population that generates the OE is increased at high temperature and the trapped electron spin population, that generates the SE, is increased at low temperature as proposed previously for linear PA.³⁵ Estimation of the SE signal enhancement requires knowledge of the electron spin relaxation times at the experimental magnetic field (14.1 T), accurate measurements of the diffusion coefficient, $D_{f/f}$, and the density of localized spins and their energetic depth. Since accurate values for these parameters are unavailable, we are unable to predict these enhancements. This is discussed in more detail in the SI.

MAS-DNP experiments were repeated on multiple cyclic PA samples prepared and isomerized under various conditions. The observed enhancements all fell within the range of \sim 30-36 and T_B ranged from 0.25 to 0.5 s at room temperature (see Table S1). In Table 1 we report the results for two cyclic PA samples at RT and 100 K that led to the largest nuclear polarization buildup times difference (0.5 s vs 1 s). This difference can be explained, in part, to different concentrations of conduction electrons (see fig S2) but also other factors yet to be determined.

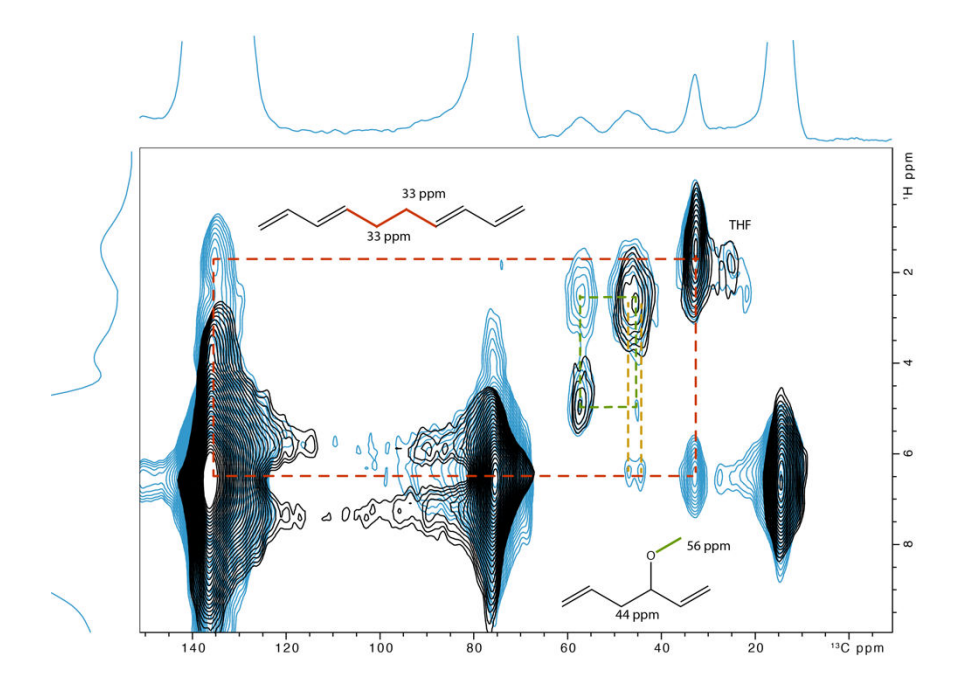
Importantly, these significant enhancements enabled for the first time the collection of ¹H-¹³C Cross-Polarization (CP)⁵⁵ spectra at both temperatures with very high sensitivity. The cyclic PA ¹³C NMR spectra at room temperature, with and without µw irradiation (at the maximum OE position), are reported in Figure 2 (b). It is important to note the spectra at room temperature and 100 K are near identical (see Fig. S.4). Despite the higher enhancement at room temperature, the higher spin polarization and the better signal-to-noise performance of the NMR probe, the

sensitivity remains better at the lowest temperature. The combination of high magnetic field and high signal-to-noise enabled the recording of ¹³C signals from defect sites in the 0 to ~100 ppm chemical shift range on the neat samples. Previous low field DNP studies attempted to identify the chemical structure of defects of linear PA under oxidative condition, but the lack of resolution in that work made the assignment challenging.³⁴ Here we take advantage of the high resolution and very high sensitivity to address two key questions about these cyclic PA samples. Firstly, can we confirm that the chains are indeed cyclic? Secondly, what defects are observed in the neat sample?

The 1D ¹³C NMR spectrum is dominated by the -CH=CH- signal at 136.5 ppm originating from the main chain. However, resonances at 25, 33, 46, 48, and 56 ppm are also clearly visible and correspond to various types of "defects". Those defect signals are enhanced by the same amount as the main chain signals which indicates a close spatial proximity with the main polymers. These signals are confirmed by spectra at different MAS rates at 100 K or at room temperature (see S.I.). These signals are different than those observed in linear PA (see S.I.). The presence of signals in the 15-20 ppm range, typically associated with -CH₃, is observed for the linear PA but is absent for the cyclic PA (see Fig S4). Such methyl groups are associated with chain termination,³⁴ and their absence is consistent with a closed cycle PA chain topology. The signal at ~25 ppm/1.8 ppm (¹³C/¹H chemical shift) may correlate with the main chain but is more likely to be indicative of tetrahydrofuran solvent molecules that can remain trapped in the polymer after synthesis.

Assignment of the additional signals based on the 1D spectra is not possible or at least ambiguous. Therefore, we took advantage of the high sensitivity to carry out ${}^{1}\text{H-}{}^{13}\text{C}$ correlation experiments with different CP times to assess the proximity of the sites to solitons. Figure 3 reports the correlations obtained using a contact time of 40 µs and 400 µs. In the first case, the spin diffusion among ${}^{1}\text{H}$ nuclear spins during CP is minimal and thus no long range correlations are observed.

For the longer CP time, the spin diffusion among proximal ¹H nuclear spins, enables probing of the chemical nature of the ¹H surrounding the ¹³C sites. Based on this approach, the signals at 33 ppm (1.8-2 ppm in the ¹H frequency dimension) correlate with the main peak at 136.5 ppm. These carbons belong to the main chain and their chemical shift indicates they are saturated sites =CH-CH₂-CH₂-CH= as shown in Figure 3. The signals at 46 and 48 ppm correlate with the main signals at 136.5 ppm. This indicates that these carbons are close to the main chain. However, the lower cross peak intensity indicates that these sites are further away from the main chain. Finally, the peak at 56 ppm only correlates with the signal at 46 ppm but not the main chain. This site is thus even further away from the main chain as it does not correlate with it. Based on the chemical shifts, these sites could be CH₃-O- that are connected to the main chain via an unsaturated site -CH-resonating at 46 ppm. Such a site would be the result of partial oxidation on the sample's surface. It is nonetheless difficult to attribute the signal with full confidence.



·

Figure 3 ¹H-¹³C correlation for cyclic PA using two different cross-polarization contact times, 40 μs (black) and 400 μs (blue). Spectra were collected at 100 K and 9.2 kHz.

In summary, this study establishes the feasibility of DNP on conductive polymers at very high magnetic fields, utilizing solitons as a nuclear hyperpolarization source. The experiments, performed on linear PA and the recently synthesized cyclic PA, revealed a remarkable enhancement which is attributed to the Overhauser effect (OE) originating from the solitons, which intriguingly persists even at room temperature where an enhancement factor of 45 was reached, a record for intrinsic defects under such magnetic field.

The combination of enhanced sensitivity and high resolution was instrumental in determining the structural composition of the defects in cyclic PA. Notably, the absence of methyl groups within the cyclic PA is unveiled, further confirming its inherent cyclic nature, and excluding the presence of detectable linear chains. This achievement not only advances our understanding of cyclic PA but also establishes a pathway towards the comprehensive analysis of conductive polymers, which are pivotal components in the landscape of molecular electronics and optoelectronics.¹

ASSOCIATED CONTENT

Experimental details and associated content are available in the Supporting Information: solitonsOEhighfieldRT-SI.pdf

AUTHOR INFORMATION

Corresponding Author

Frédéric Mentink-Vigier National High Magnetic Field Laboratory, Florida State University, 1800 E. Paul Dirac Dr, Tallahassee, FL, 32310, USA. ORCID: 0000-0002-3570-9787, Email: fmentink@magnet.fsu.edu

Authors

Zhihui Miao: Department of Chemistry, University of Florida, Center for Catalysis, PO Box 117200, Gainesville, FL 32611-7200 USA. Email: zmiao@mmm.com

Faith J. Scott: National High Magnetic Field Laboratory, Florida State University, 1800 E. Paul Dirac Dr, Tallahassee, FL, 32310, USA. ORCID: <u>0000-0003-3903-8842</u>, Email: <u>fscott@magnet.fsu.edu</u>

Johan van Tol: National High Magnetic Field Laboratory, Florida State University, 1800 E. Paul Dirac Dr, Tallahassee, FL, 32310, USA. ORCID: 0000-0001-6972-2149, Email: fscott@magnet.fsu.edu

Clifford R. Bowers: Department of Chemistry and National High Magnetic Field Lab, University of Florida, PO Box 117200, Gainesville, FL 32611-7200 USA. ORCID: 0000-0001-6155-5163, Email: bowers@chem.ufl.edu

Adam S. Veige: Department of Chemistry, University of Florida, Center for Catalysis, PO Box 117200, Gainesville, FL 32611-7200 USA. ORCID: 0000-0002-7020-9251, Email: veige@chem.ufl.edu

ACKNOWLEDGMENTS

The National High Magnetic Field Laboratory (NHMFL) is funded by the National Science Foundation Division of Materials Research (DMR-1644779 and DMR-2128556) and the State of Florida. A portion of this work was supported by the NIH RM1-GM148766 and the European Union's Horizon 2020 Research and Innovation Programme under grant agreement no. 101008500. FJS acknowledges support from a Diversity Postdoctoral Scholar award from the Provost's Office at Florida State University. CRB acknowledges support from NSF grants CHE-2108306 and CBET-1933723. ASV acknowledges support from NSF grant CHE-2108266.

REFERENCES

- 1 T. Nezakati, A. Seifalian, A. Tan and A. M. Seifalian, Conductive Polymers: Opportunities and Challenges in Biomedical Applications, *Chem. Rev.*, 2018, **118**, 6766–6843.
- 2 G. Natta, G. Mazzanti and P. Corradini, Atti Accad. Naz. Lincei, Cl, Sci. Fis. Mat. Nat., Rend.
- 3 T. Ito, H. Shirakawa and S. Ikeda, Simultaneous polymerization and formation of polyacetylene film on the surface of concentrated soluble Ziegler-type catalyst solution, *J. Polym. Sci. Polym. Chem. Ed.*, 1974, **12**, 11–20.
- 4 H. Shirakawa and S. Ikeda, Infrared Spectra of Poly(acetylene), *Polym J*, 1971, **2**, 231–244.
- 5 H. Shirakawa, E. J. Louis, A. G. MacDiarmid, C. K. Chiang and A. J. Heeger, Synthesis of electrically conducting organic polymers: halogen derivatives of polyacetylene, (CH) x, *J. Chem. Soc., Chem. Commun.*, 1977, 578.
- 6 C. K. Chiang, C. R. Fincher, Y. W. Park, A. J. Heeger, H. Shirakawa, E. J. Louis, S. C. Gau and A. G. MacDiarmid, Electrical Conductivity in Doped Polyacetylene, *Phys. Rev. Lett.*, 1977, **39**, 1098–1101.
- 7 J. C. W. Chien, F. E. Karasz and G. E. Wnek, Soliton formation and cis trans isomerization in polyacetylene, *Nature*, 1980, **285**, 390–392.
- 8 Z. Miao, S. A. Gonsales, C. Ehm, F. Mentink-Vigier, C. R. Bowers, B. S. Sumerlin and A. S. Veige, Cyclic polyacetylene, *Nat. Chem.*, 2021, **13**, 792–799.
- 9 Z. Miao, A. M. Esper, S. S. Nadif, S. A. Gonsales, B. S. Sumerlin and A. S. Veige, Semiconducting cyclic copolymers of acetylene and propyne, *Reactive and Functional Polymers*, 2021, **169**, 105088.
- 10Z. Miao, D. Konar, B. S. Sumerlin and A. S. Veige, Soluble Polymer Precursors via Ring-Expansion Metathesis Polymerization for the Synthesis of Cyclic Polyacetylene, *Macromolecules*, 2021, **54**, 7840–7848.
- 11 V. K. Jakhar, Y.-H. Shen, S.-M. Hyun, A. M. Esper, I. Ghiviriga, K. A. Abboud, D. W. Lester and A. S. Veige, Improved Trianionic Pincer Ligand Synthesis for Cyclic Polymer Catalysts, *Organometallics*, 2023, **42**, 1339–1346.
- 12S. Kuppuswamy, A. J. Peloquin, I. Ghiviriga, K. A. Abboud and A. S. Veige, Synthesis and Characterization of Tungsten(VI) Alkylidene Complexes Supported by an [OCO] ³⁻ Trianionic

- Pincer Ligand: Progress towards the [^t BuOCO]W≡CC(CH₃)₃ Fragment, *Organometallics*, 2010, **29**, 4227–4233.
- 13 K. P. McGowan, M. E. O'Reilly, I. Ghiviriga, K. A. Abboud and A. S. Veige, Compelling mechanistic data and identification of the active species in tungsten-catalyzed alkyne polymerizations: conversion of a trianionic pincer into a new tetraanionic pincer-type ligand, *Chem. Sci.*, 2013, 4, 1145–1155.
- 14C. D. Roland, H. Li, K. A. Abboud, K. B. Wagener and A. S. Veige, Cyclic polymers from alkynes, *Nature Chem*, 2016, **8**, 791–796.
- 15S. Sarkar, K. P. McGowan, S. Kuppuswamy, I. Ghiviriga, K. A. Abboud and A. S. Veige, An OCO ^{3–} Trianionic Pincer Tungsten(VI) Alkylidyne: Rational Design of a Highly Active Alkyne Polymerization Catalyst, *J. Am. Chem. Soc.*, 2012, **134**, 4509–4512.
- 16A. S. Lilly Thankamony, J. J. Wittmann, M. Kaushik and B. Corzilius, Dynamic nuclear polarization for sensitivity enhancement in modern solid-state NMR, *Progress in Nuclear Magnetic Resonance Spectroscopy*, 2017, 102–103, 120–195.
- 17A. G. M. Rankin, J. Trébosc, F. Pourpoint, J.-P. Amoureux and O. Lafon, Recent developments in MAS DNP-NMR of materials, *Solid State Nuclear Magnetic Resonance*, 2019, **101**, 116–143.
- 18D. Lee, S. Hediger and G. De Paëpe, Is solid-state NMR enhanced by dynamic nuclear polarization?, *Solid State Nuclear Magnetic Resonance*, 2015, **66–67**, 6–20.
- 19B. Reif, S. E. Ashbrook, L. Emsley and M. Hong, Solid-state NMR spectroscopy, *Nat Rev Methods Primers*, 2021, **1**, 1–23.
- 20A. J. Rossini, A. Zagdoun, M. Lelli, A. Lesage, C. Coperet and L. Emsley, Dynamic nuclear polarization surface enhanced NMR spectroscopy., *Accounts of chemical research*, 2013, **46**, 1942–51.
- 21T. Maly, G. T. Debelouchina, V. S. Bajaj, K.-N. Hu, C.-G. Joo, M. L. Mak-Jurkauskas, J. R. Sirigiri, P. C. A. van der Wel, J. Herzfeld, R. J. Temkin and R. G. Griffin, Dynamic nuclear polarization at high magnetic fields., *J. Chem. Phys.*, 2008, **128**, 052211.
- 22M. A. Hope, B. L. D. Rinkel, A. B. Gunnarsdóttir, K. Märker, S. Menkin, S. Paul, I. V. Sergeyev and C. P. Grey, Selective NMR observation of the SEI–metal interface by dynamic nuclear polarisation from lithium metal, *Nat Commun*, 2020, **11**, 2224.
- 23M. Lelli, S. R. Chaudhari, D. Gajan, G. Casano, A. J. Rossini, O. Ouari, P. Tordo, A. Lesage and L. Emsley, Solid-State Dynamic Nuclear Polarization at 9.4 and 18.8 T from 100 K to Room Temperature, *J. Am. Chem. Soc.*, 2015, **137**, 14558–14561.
- 24M. A. Hope, S. Björgvinsdóttir, D. M. Halat, G. Menzildjian, Z. Wang, B. Zhang, J. L. MacManus-Driscoll, A. Lesage, M. Lelli, L. Emsley and C. P. Grey, Endogenous ¹⁷ O Dynamic Nuclear Polarization of Gd-Doped CeO ₂ from 100 to 370 K, *J. Phys. Chem. C*, 2021, **125**, 18799–18809.
- 25D. A. Hall, D. C. Maus, G. J. Gerfen, S. J. Inati, L. R. Becerra, F. W. Dahlquist and R. G. Griffin, Polarization-Enhanced NMR Spectroscopy of Biomolecules in Frozen Solution, *Science*, 1997, **276**, 930–932.
- 26K. R. Thurber and R. Tycko, Theory for cross effect dynamic nuclear polarization under magicangle spinning in solid state nuclear magnetic resonance: the importance of level crossings., *J. Chem. Phys.*, 2012, **137**, 084508.
- 27F. Mentink-Vigier, U. Akbey, Y. Hovav, S. Vega, H. Oschkinat and A. Feintuch, Fast passage dynamic nuclear polarization on rotating solids., *Journal of Magnetic Resonance*, 2012, **224**, 13–21.

- 28B. A. DeHaven, J. T. Tokarski, A. A. Korous, F. Mentink-Vigier, T. M. Makris, A. M. Brugh, M. D. E. Forbes, J. van Tol, C. R. Bowers and L. S. Shimizu, Persistent Radicals of Self-assembled Benzophenone bis -Urea Macrocycles: Characterization and Application as a Polarizing Agent for Solid-state DNP MAS Spectroscopy, Chem. Eur. J., 2017, 23, 8315–8319.
- 29A. Harchol, G. Reuveni, V. Ri, B. Thomas, R. Carmieli, R. H. Herber, C. Kim and M. Leskes, Endogenous Dynamic Nuclear Polarization for Sensitivity Enhancement in Solid-State NMR of Electrode Materials, *J. Phys. Chem. C*, 2020, **124**, 7082–7090.
- 30S. L. Carnahan, Y. Chen, J. F. Wishart, J. W. Lubach and A. J. Rossini, Magic angle spinning dynamic nuclear polarization solid-state NMR spectroscopy of γ-irradiated molecular organic solids, *Solid State Nuclear Magnetic Resonance*, 2022, **119**, 101785.
- 31 W. P. Su, J. R. Schrieffer and A. J. Heeger, Soliton excitations in polyacetylene, *Phys. Rev. B*, 1980, **22**, 2099–2111.
- 32M. Nechtschein, F. Devreux, F. Genoud, M. Guglielmi and K. Holczer, Magnetic-resonance studies in undoped trans-polyacetylene \${(\mathrm{CH})}_{x}\$. II, *Phys. Rev. B*, 1983, **27**, 61–78.
- 33K. Holczer, J. P. Boucher, F. Devreux and M. Nechtschein, Magnetic-resonance studies in undoped trans-polyacetylene, \${(\mathrm{CH})} {x}\$, *Phys. Rev. B*, 1981, **23**, 1051–1063.
- 34R. A. Wind, M. J. Duijvestijn and J. Vriend, Structural defects in undoped trans-polyacetylene, before and after air oxidation, studied by DNP-enhanced 13C NMR, *Solid State Communications*, 1985, **56**, 713–716.
- 35W. G. Clark, K. Glover, G. Mozurkewich, S. Etemad and M. Maxfield, Measurements of Soliton Trapping and Motion in Trans-Polyacetylene Using Dynamic Nuclear Polarization, *Molecular Crystals and Liquid Crystals*, 1985, 117, 447–454.
- 36A. Svirinovsky-Arbeli, D. Rosenberg, D. Krotkov, R. Damari, K. Kundu, A. Feintuch, L. Houben, S. Fleischer and M. Leskes, The effects of sample conductivity on the efficacy of dynamic nuclear polarization for sensitivity enhancement in solid state NMR spectroscopy, *Solid State Nuclear Magnetic Resonance*, 2019, **99**, 7–14.
- 37 V. P. Denysenkov and T. F. Prisner, in eMagRes, John Wiley & Sons, Ltd, 2019, pp. 41-54.
- 38M. Bennati and T. Orlando, Overhauser DNP in liquids on 13C nuclei, *eMagRes*, 2019, **8**, 11–18.
- 39Z. Miao, S. A. Gonsales, C. Ehm, F. Mentink-Vigier, C. R. Bowers, B. S. Sumerlin and A. S. Veige, Cyclic polyacetylene, *Nat. Chem.*, 2021, **13**, 792–799.
- 40 A. J. Heeger, S. Kivelson, J. R. Schrieffer and W.-P. Su, Solitons in conducting polymers, *Rev. Mod. Phys.*, 1988, **60**, 781–850.
- 41I. B. Goldberg, H. R. Crowe, P. R. Newman, A. J. Heeger and A. G. MacDiarmid, Electron spin resonance of polyacetylene and AsF5-doped polyacetylene, *The Journal of Chemical Physics*, 1979, **70**, 1132–1136.
- 42 S. Kuroda and H. Shirakawa, Electron-nuclear double-resonance evidence for the soliton wave function in polyacetylene, *Phys. Rev. B*, 1987, **35**, 9380–9382.
- 43 S. Jeyadev and E. M. Conwell, Soliton diffusion in trans-polyacetylene, *Phys. Rev. Lett.*, 1987, **58**, 258–261.
- 44M. Mehring, H. Seidel, W. Müller and G. Wegner, Time resolved ESR of paramagnetic defects in undoped polyacetylene, *Solid State Communications*, 1983, **45**, 1075–1077.
- 45K. Potje-Kamloth, in *Handbook of Surfaces and Interfaces of Materials*, ed. H. S. Nalwa, Academic Press, Burlington, 2001, pp. 445–494.
- 46A. Overhauser, Polarization of Nuclei in Metals, *Phys. Rev.*, 1953, **92**, 411–415.

- 47T. R. Carver and C. P. Slichter, Experimental Verification of the Overhauser Nuclear Polarization Effect, *Phys. Rev.*, 1956, **102**, 975–980.
- 48T. V. Can, M. a. Caporini, F. Mentink-Vigier, B. Corzilius, J. J. Walish, M. Rosay, W. E. Maas, M. Baldus, S. Vega, T. M. Swager and R. G. Griffin, Overhauser effects in insulating solids, *The Journal of Chemical Physics*, 2014, **141**, 064202.
- 49R. A. Wind, M. J. Duijvestijn, C. van der Lugt, A. Manenschijn and J. Vriend, Applications of dynamic nuclear polarization in 13C NMR in solids, *Prog. Nucl. Magn. Reson. Spectrosc.*, 1985, 17, 33–67.
- 50 Y. Hovav, A. Feintuch and S. Vega, Theoretical aspects of dynamic nuclear polarization in the solid state the solid effect., *J. Magn. Reson.*, 2010, **207**, 176–89.
- 51M. Nechtschein, F. Devreux, R. L. Greene, T. C. Clarke and G. B. Street, One-Dimensional Spin Diffusion in Polyacetylene, \${(\mathrm{CH})}_{x}\$, *Phys. Rev. Lett.*, 1980, **44**, 356–359.
- 52G. Völkel, S. A. Dzuba, A. Bartl, W. Brunner and J. Fröhner, Time-Resolved EPR on Polyacetylene, *physica status solidi (a)*, 1984, **85**, 257–263.
- 53K. Holczer, F. Devreux, M. Nechtschein and J. P. Travers, Spin dynamics at low temperature in undoped trans-polyacetylene, (CH)x, *Solid State Communications*, 1981, **39**, 881–884.
- 54W. G. Clark, K. Glover, G. Mozurkewich, C. T. Murayama, J. Sanny, S. Etemad and M. Maxfield, ELECTRON SPIN MOTION IN TRANS-(CH) x, *J. Phys. Colloques*, 1983, 44, C3-239-C3-245.
- 55 A. Pines, M. G. Gibby and J. S. Waugh, Proton-enhanced NMR of dilute spins in solids, *The Journal of Chemical Physics*, 1973, **59**, 569–590.